JOURNAL OF MATERIALS SCIENCE 28 (1993) 1415–1420

Effect of microstructure on the hardness and fracture toughness of $YBa_2Cu_3O_{7-x}$/Ag composites

W. H. TUAN, J. M. WU
Institute of Materials Science and Engineering, National Taiwan University, Taipei, Taiwan 10764

Applications of $YBa_2Cu_3O_{7-x}$ (Y123) superconducting ceramic are often handicapped by the problems associated with its poor mechanical performance. In the present study, silver inclusions were introduced into the Y123 matrix and the effects of microstructure on the hardness and the fracture toughness of the composites were investigated. The results revealed that the hardness of the composites depends strongly on the amount of porosity and the silver content, and that the fracture toughness also depends on the silver content. Both hardness and fracture toughness exhibit a strong dependence on the inter-connectivity of the silver inclusions. As the amount of interconnected silver is increased, the hardness becomes less sensitive to the existence of porosity and the toughness is enhanced. The composites are therefore more tolerant to intrinsic flaws than is the matrix alone.

1. Introduction

The mechanical performance of ceramics generally exhibits a complex dependence on microstructure. Regardless of whether ceramic superconductors are used for their unique superconducting properties, the prevention of mechanical failure is a most important, if not critical, requirement. The ceramic superconducting $YBa_2Cu_3O_{7-x}$ compound, commonly known as "Y123", has received much attention because of its high critical temperature, T_c. However, previous research has shown that the mechanical properties of Y123 compounds are generally rather poor, especially with an unacceptably low fracture toughness. For example, fracture toughness results by the indentation method indicate values of 1.3 MPa $m^{0.5}$ for polycrystalline Y123 [1], and 1.1 and 0.43 MPa $m^{0.5}$ for single crystals [2, 3]; results from single edge-notched beam (SENB) tests indicate a value of 1.1 MPa $m^{0.5}$ for polycrystalline Y123 [4].

For other ceramics, a major research objective has been to improve the fracture toughness. The addition of second-phase inclusions which influence the propagation of cracks has been much studied. Inclusions which induce transformation toughening or toughening by microcracking have produced dramatic benefits [5–7]. Ceramic inclusions whose strength is higher than that of the ceramic matrix have been used as reinforcements; for example, SiC whiskers in an alumina matrix have been found to be beneficial [8], although considerable difficulties can be experienced in the processing of such whisker composites.

Toughening ceramics by ductile inclusions is also of considerable interest. This approach has recently been successfully applied to several ceramic oxide systems, for example aluminium-toughened glass [9], aluminium-toughened alumina [10] and nickel-toughened alumina [11]. Previous studies have indicated that crack bridging is usually the strongest mechanism [10–12]. This approach has also been successfully applied to ceramic superconductors (Table I) [13–15].

The reported values for the hardness of Y123 and Y123/Ag composites are shown in Table II [13, 16]. As with values of fracture toughness, the reported data are widely scattered. Furthermore, the effect of microstructure on the mechanical properties has not been thoroughly studied. In order to optimize the mechanical performance of a composite, the microstructure must be tailored. In the present study, the effect of the microstructural parameters (density, inclusion content, size of inclusion and the distribution of inclusions) on the mechanical properties (hardness and toughness) of Y123/Ag composites were investigated.

2. Experimental procedure

The Y123 powder was prepared by the solid-state reaction of the constituent oxides Y_2O_3, CuO and BaO. Powdered Y_2O_3, CuO and $BaCO_3$ were mixed in appropriate proportions and ball milled in ethyl alcohol for 24 h using zirconia balls as the grinding medium. The slurry was dried with a rotary evaporator. The powder mixtures were then calcined at 950 °C for 12 h, and annealed at 480 °C for 8 h in a flowing oxygen atmosphere. The calcined lumps were ball milled in ethyl alcohol for 24 h. The slurry was allowed to settle for 10 min and the suspension was collected and then dried. The dried lumps were crushed and passed through a plastic sieve with aperture

0022–2461

TABLE I The fracture toughness of Y123/Ag composites from other studies

K_{IC} for 15% Ag composite (MPa $m^{0.5}$)	$\frac{K_{IC}}{K_{IC,Y123}}$	Relative density (%)	Inclusion size (μm)	Measurement method	Reference
1.4	1.5	91	2–3.5[a]	SENB	[13]
2.0	1.9	87	NA[b]	SENB	[14]
3.3	2.8	95	3[a]	SENB	[15]
2.4	2.2	90	3.2	Indentation	Present work

[a] Initial inclusion size.
[b] NA, not available.

TABLE II The hardness of Y123 and Y123/Ag composites from other studies

Composition	Hardness (GPa)	Relative density (%)	Inclusion size (μm)	Reference	Comments
Y123	1.37	85	–	[13]	Polycrystal
Y123/15 vol % Ag	1.60	91	2–3.5[a]	[13]	Polycrystal
Y123	10.3	NA[b]	–	[16]	Polycrystal

[a] Initial inclusion size.
[b] NA, not available.

size 0.074 mm. The average particle size of the resulting Y123 powder was 0.92 μm.

The Y123/Ag composites were prepared by ball milling various amounts of Ag_2O with the Y123 powder for 24 h. The resulting composition contained 5–20 vol % Ag after sintering. The powder mixtures were dried and sieved. Specimens, 1 cm diameter and 0.3–0.4 cm high, were prepared by uniaxially pressing at 200 MPa in a steel mould. The samples were sintered in a flowing oxygen atmosphere in the temperature range 900–950 °C and then annealed at 480 °C. The samples were heated slowly to 350 °C at a heating rate of 0.5 °C min^{-1}. The specimens were held at that temperature for 3 h. The heating rate between 350 °C and the sintering temperature was 5 °C min^{-1}. The cooling rate between the sintering temperature and 480 °C was 3 °C min^{-1}. After annealing at 480 °C for 8 h, the samples were cooled to room temperature at 2 °C min^{-1}.

Bulk density was determined by measuring the weight and the dimensions of the samples. By assuming the reaction between Y123 and silver is limited [17], the relative densities of the composites were estimated by the rule of mixtures with a theoretical density of 6.38 g cm^{-3} for Y123 and 10.5 g cm^{-3} for silver. Phase identification was performed by X-ray diffractometry (Phillips PW1729, Phillips Co., The Netherlands). Polished surfaces were prepared by polishing with 6 and 1 μm diamond particles and 0.05 μm alumina paste. The microstructure of the composites was observed by reflected polarized light microscopy. The inclusion size was determined by a linear intercept technique [18].

Mechanical failure characteristics in the composites were investigated by examining indentation-induced cracks by scanning electron microscopy (SEM). The connectivity of the silver inclusions within the matrix was determined by measuring the electrical resistivity at room temperature. The resistivity was measured by the standard d.c. four-probe technique, using silver paint for the contacts.

A number of testing techniques could be used to characterize the fracture toughness of ceramics, including SENB, chevron-notched beam (CNB), indentation, etc. However, none of these techniques was regarded as giving more reliable results than the others. Although the indentation technique used in the present work may not be better in terms of giving absolute fracture toughness values than other techniques such as SENB and CNB, it could provide a great deal of information on the effect of microstructure on mechanical properties and on the dominant toughening mechanism of the composites. Indentation was performed with a Vickers microhardness tester (MS-55, Akashi Co., Japan). To determine hardness, a 1 N load was applied. For fracture toughness, a 10 N load was applied to obtain long, clear cracks. The relationship proposed by Anstis *et al.* [19]

$$K_{IC} = 0.016\,(E/H)^{0.5}\,(P/c^{1.5}) \quad (1)$$

was used to calculate values of fracture toughness, K_{IC}, where E is the elastic modulus, H the hardness, P the load applied and c the average radial crack length. In order to determine reliable values, the measurement of fracture toughness was only performed on specimens with a relative density above 86%.

3. Results and discussion

The X-ray diffraction patterns of the sintered composites were compared with the published patterns [20] and identified as mixtures of orthorhombic $YBa_2Cu_3O_{7-x}$ and cubic silver. The relative density and the size of the silver inclusions in the composites containing various amount of silver are shown as a function of sintering temperature and time in Table III. Typical microstructures of Y123 and Y123/Ag composites are shown in Fig. 1a, and b,

TABLE III The relative density, inclusion size, hardness, fracture toughness and normalized resistivity for Y123 and Y123/Ag composites

Sintering conditions (°C)	(min)	Silver content (%)	Relative density (%)	Inclusion size (μm)	Hardness (GPa)	Toughness (MPa $m^{0.5}$)	Normalized resistivity
900	360	0	65.1	–	1.13	–	1.0
		5	70.6	0.53	1.51	–	0.90
		10	65.5	0.66	1.45	–	0.68
		15	70.2	0.90	1.79	–	0.54
		20	64.3	1.03	1.55	–	0.38
920	360	0	74.2	–	2.51	–	1.0
		5	81.6	1.66	1.76	–	0.87
		10	83.7	1.81	1.81	–	0.65
		15	84.5	2.26	2.15	–	0.40
		20	86.2	2.54	2.34	2.4	0.21
930	360	0	79.9	–	3.31	–	1.0
		5	84.5	1.73	3.55	–	0.88
		10	86.0	1.92	2.87	–	0.59
		15	86.6	2.34	2.67	2.2	0.38
		20	89.1	2.67	2.57	2.7	0.20
940	360	0	86.7	–	4.35	1.1	1.0
		5	90.8	1.81	4.02	1.5	0.82
		10	89.9	2.50	3.11	2.1	0.56
		15	90.2	2.44	2.92	2.4	0.35
950	360	0	88.2	–	4.14	1.1	1.0
		5	88.4	5.02	3.83	1.4	0.84
		10	88.0	5.08	3.06	1.8	0.54
930	1	0	65.6	–	1.05	–	–
		5	73.5	0.52	1.42	–	–
		10	70.2	0.56	1.21	–	–
		15	69.6	1.12	1.03	–	–
		20	62.6	1.17	0.65	–	–
930	10	0	67.1	–	1.54	–	–
		5	75.1	0.60	1.60	–	–
		10	71.1	0.80	1.48	–	–
		15	71.5	1.21	1.16	–	–
		20	63.2	1.46	0.96	–	–
930	100	0	74.3	–	2.43	–	1.0
		5	75.4	0.92	2.27	–	0.91
		10	80.0	1.68	2.29	–	0.69
		15	81.5	1.78	2.21	–	0.42
		20	88.5	2.35	2.45	2.6	0.22
930	1000	0	94.1	–	4.54	1.1	1.0
		5	90.2	5.33	3.98	1.5	0.85
		15	90.7	2.86	2.78	2.4	0.35
		20	90.4	3.11	2.64	2.8	0.20
930	5000	0	95.7	–	4.65	1.2	1.0
		5	90.5	7.45	3.57	1.4	0.84
		10	91.4	4.01	3.18	1.9	0.52
		15	94.0	3.00	3.17	2.0	0.32
		20	93.5	3.23	2.85	2.3	0.19

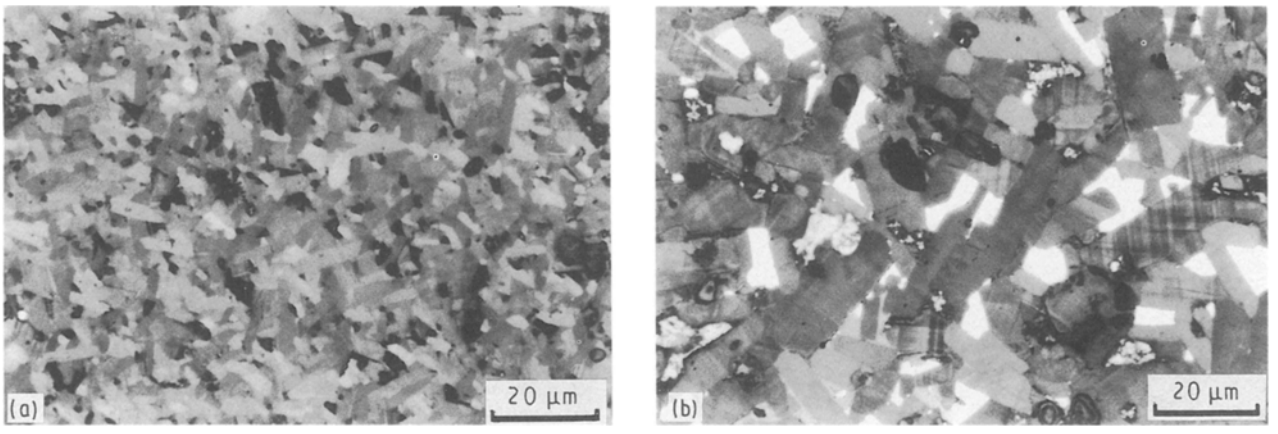

Figure 1 Typical microstructures of (a) Y123 and (b) Y123/5 vol % Ag composite. Samples were sintered at 950 °C for 360 min.

respectively. The composite shown in Fig. 1b, contains 5 vol % silver. Both samples were sintered at 950 °C for 360 min. Fig. 1b shows that the silver particles are well distributed within the matrix.

The normalized resistivity is shown in Fig. 2 as a function of effective silver content, which is the product of the expected silver content for a fully dense composite and the relative density. The normalized resistivity calculated by the rule of mixtures (ROM) is also shown in the figure. The values of the measured resistivity are lower than that predicted by the ROM, suggesting that some silver inclusions are interconnected within the Y123 matrix. As the effective silver content is increased, i.e. either the amount of added silver or the relative density is increased, the amount of interconnected silver inclusions is correspondingly increased. The temperature dependence of the resistivity reveals that the zero-resistivity for the composite containing 18 vol % effective silver content is 86 K, thus indicating that the Y123 grains within the composites also form interconnected networks.

The hardness of the samples is shown as a function of porosity in Fig. 3. The hardness of pure Y123 and Y123/Ag composites is seen to exhibit an exponential relationship with the porosity

$$H = H_0 \exp(-bP) \quad (2)$$

where H is the hardness, H_0 the hardness for the fully dense sample (6.9 GPa in the present study), P the porosity and b a constant. Such a relationship can also be found for other ceramics. For most ceramics, b varies from 3–9 [21]. The value of 4.9 for pure Y123 obtained in the present study lies within this range, Fig. 3a. The constants for composites containing various amounts of silver also fall within the range, Fig. 3b. Furthermore, b decreased with increasing silver content, suggesting that the toughness of the composites depends strongly on the distribution of the silver inclusions. Because the composites contain more ductile inclusions, the hardness is less sensitive to the existence of intrinsic flaws (porosity).

To investigate the effect of silver content on hardness, the hardness of the samples with relative density varying from 86%–94% is shown as a function of effective silver content in Fig. 4. The hardness is decreased with increasing effective silver content.

The fracture toughness is shown as a function of relative density and effective silver content in Figs 5 and 6, respectively. The fracture toughness is not sensitive to change in relative density; however, it does show a significant increase with increasing effective silver content. For a composite containing 18 vol % effective silver inclusion, the fracture toughness is 2.5 times that of Y123 alone.

From Fig. 5, the fracture toughness for the composites is seen to increase slightly initially then de-

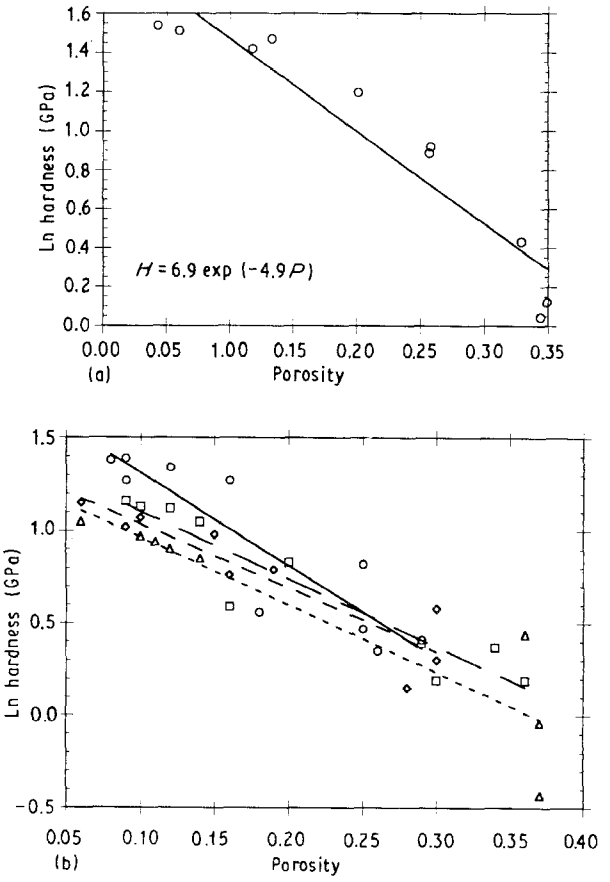

Figure 3 The natural logarithm values of hardness as a function of porosity for (a) Y123, (b) Y123/Ag composites: (○) 5% Ag, $H = 6.2 \exp(-5.0P)$, (□) 10% Ag, $H = 4.3 \exp(-3.6P)$, (◇) 15% Ag, $H = 4.0 \exp(-3.5P)$, (△) 20% Ag, $H = 3.8 \exp(-3.7P)$.

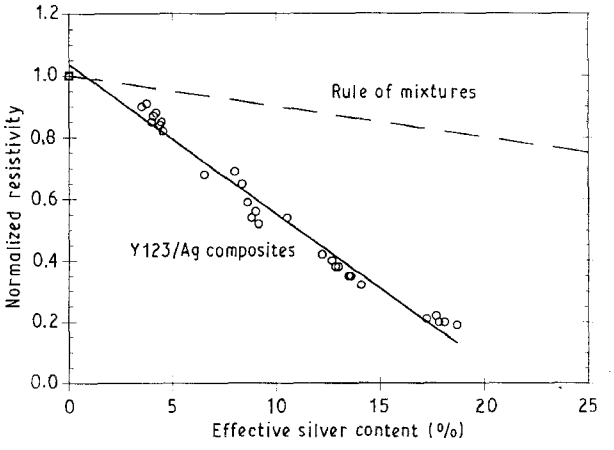

Figure 2 The normalized resistivity as a function of effective silver content.

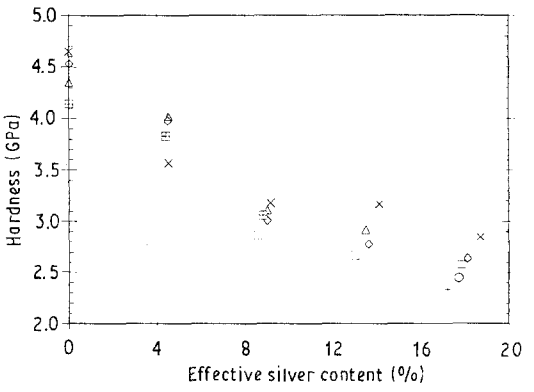

Figure 4 The hardness as a function of effective silver content. The relative density varied from 86%–94%. (○) 930 °C, 100 min; (·) 930 °C, 360 min; (◇) 930 °C, 1000 min; (×) 930 °C, 5000 min; (+) 920 °C, 360 min; (△) 940 °C, 360 min; (⊞) 950 °C, 360 min.

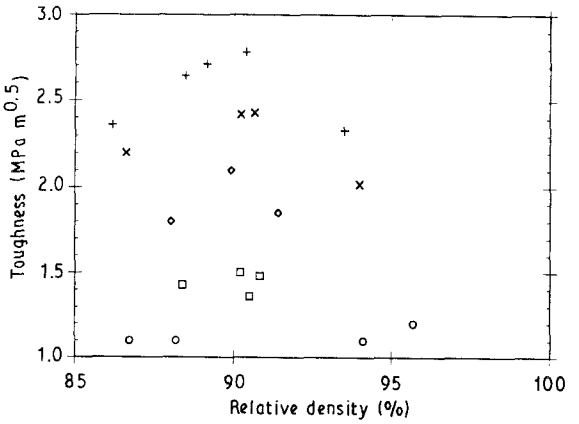

Figure 5 The fracture toughness as a function of relative density. The composites containing the indicated silver fractions were sintered at various temperatures and times. (○) 0% Ag, (□) 5% Ag, (◇) 10% Ag, (×) 15% Ag, (+) 20% Ag.

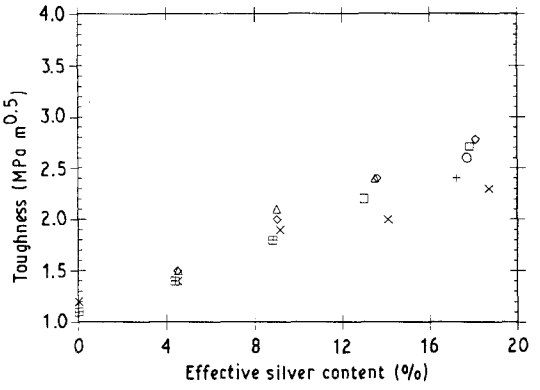

Figure 6 The fracture toughness as a function of effective silver content. The relative density varied from 86%–94%. (○) 930 °C, 100 min; (□) 930 °C, 360 min; (◇) 930 °C, 1000 min; (×) 930 °C, 5000 min; (+) 920 °C, 360 min; (△) 940 °C, 360 min; (⊞) 950 °C, 360 min.

crease at the end. This may be related to a critical inclusion size concept [22]. Because the thermal expansion coefficient of silver (22 M K^{-1}) is higher than that of Y123 (11.5 M K^{-1}) [4], a radial tensile stress is induced at the interface and may generate a circumferential crack when the silver particle size exceeds a critical size. By applying the methodology proposed by Davidge and Green [23], 3.1 μm is obtained as the critical size, which is very close to that observed in the present study (Table I).

From microstructural observation of the interactions between the crack and the silver particles, the crack may either propagate along the interface, or bypass the bridging particle (Fig. 7). This suggests that the toughening mechanism of the composites involves the plastic deformation of the metal particles. According to the theoretical predictions proposed by Ashby *et al.* [12], the increase in toughness is proportional to the square root of the product of volume fraction and inclusion size

$$\Delta K_{IC} = A\,(Fd)^{1/2} \qquad (3)$$

where ΔK_{IC} is the toughness increase, A is constant which depends on the interfacial strength, the elastic modulus and the yield strength of the ductile phase, F is the volume fraction, and d the inclusion size. The experimental results for the composites are compiled in Fig. 8; the expected linear relationship is indeed found. The fracture toughness of the composites also exhibits a strong dependence on the interconnectivity of the silver inclusions, Fig. 9. As more ductile inclusions become interconnected, the crack can not bypass the inclusions; the active (or effective) inclusions are thus increased, as with the fracture toughness.

4. Conclusion

Y123/Ag composites were prepared by sintering powdered mixtures of Y123 and Ag_2O. The brittle

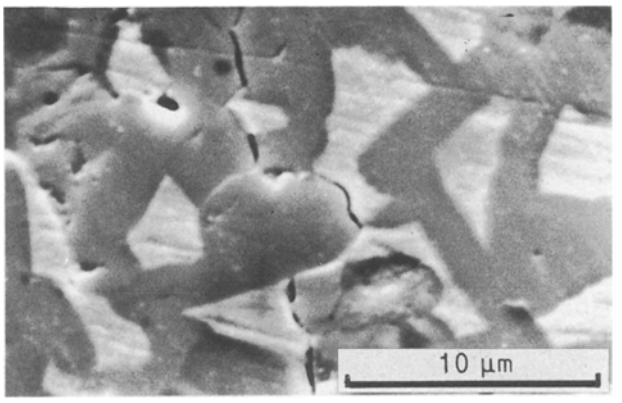

Figure 7 Bridging silver particles observed on the polished surface.

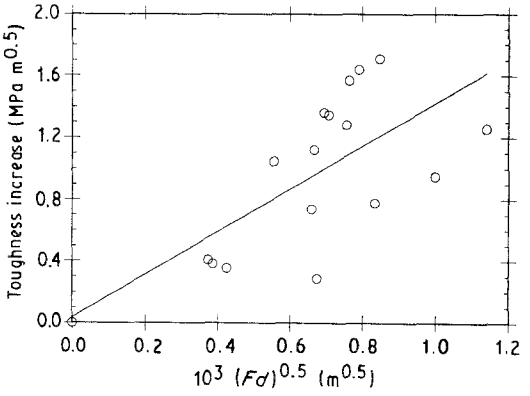

Figure 8 The increase in fracture toughness of Y123/Ag composites as a function of the square root of the product of volume fraction and inclusion size.

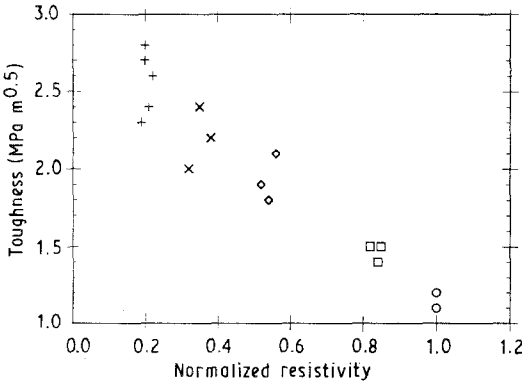

Figure 9 The fracture toughness as a function of normalized resistivity. (○) 0% Ag, (□) 5% Ag, (◇) 10% Ag, (×) 15% Ag, (+) 20% Ag.

Y123 was toughened by the addition of silver inclusions. For the composite containing 18 vol % effective silver inclusion, the fracture toughness was found to be 2.5 times that of Y123 alone. As the effective silver content was increased, the interconnected silver inclusions were increased, and also the fracture toughness of the composites. For the composites containing more interconnected inclusions, the dependence of the hardness on porosity was reduced. Therefore, the Y123/Ag composites with interconnected ductile networks are much more tolerant to intrinsic flaws.

From microstructural observations, strained silver particles are observed to bridge crack surfaces in the polished section, suggesting that the toughening mechanism of the composites is by bridging. The experimental results for the toughness increase are consistent with the theoretical predictions of Ashby *et al.* [12]. The following guidelines for manufacturing Y123/Ag composites can thus be suggested. The toughened Y123 should have: (1) a higher volume fraction of ductile inclusions, (2) a larger inclusion size (but smaller than the critical size), and (3) interconnected inclusions.

Acknowledgements

This work was supported by the National Science Council, Taiwan, under Contract NSC80-0405-E002-09. The authors thank Professor J. Wei for helpful comments.

References

1. R. F. COOK, T. M. SHAW and P. R. DUNCOMBE, *Adv. Ceram. Soc.* **2** (1987) 606.
2. R. F. COOK, T. R. DINGER and D. R. CLARK, *Appl. Phys. Lett.* **51** (1987) 454.
3. V. V. DEMIRSKII, H. J. KAUFMANN, S. V. LUBENETS, V. D. NATSIL and L. S. FOMENKO, *Sov. Phys. Solid State* **31** (1989) 1065.
4. N. McN. ALFORD, J. D. BIRCHALL, W. J. CLEGG, M. A. HARMER, K. KENDALL and D. H. JONES, *J. Mater. Sci.* **23** (1988) 761.
5. A. H. HEUER and L. W. HOBBS (eds), "Science and Technology of Zirconia I", Advances in Ceramics, Vol. 3 (American Ceramic Society, Columbus, OH, 1981).
6. N. CLAUSSEN, M. RUEHLE and A. H. HEUER (eds), "Science and Technology of Zirconia II", Advances in Ceramics, Vol. 10 (American Ceramic Society, Columbus, OH, 1984).
7. S. SOMIYA, N. YAMAMOTO and H. YANAGIDA (eds), "Science and Technology of Zirconia III", Advances in Ceramics, Vol. 24 (American Ceramic Society, Columbus, OH, 1988).
8. G. C. WEI and P. F. BECHER, *Amer. Ceram. Soc. Bull.* **64** (1985) 298.
9. V. V. KRSTIC, P. S. NICHOLSON and R. G. HOAGLAND, *J. Amer. Ceram. Soc.* **64** (1981) 499.
10. B. D. FLINN, M. RUEHLE and A. G. EVANS, *Acta Metall.* **37** (1989) 3001.
11. W. H. TUAN and R. J. BROOK, *J. Eur. Ceram. Soc.* **6** (1990) 31.
12. A. F. ASHBY, F. J. BLUNT and M. BANNISTER, *Acta Metall.* **37** (1989) 1847.
13. J. P. SINGH, H. J. LEU, R. B. POEPPEL, E. VAN VOORHEES, G. T. GOUDEY, K. WINSLEY and D. SHI, *J. Appl. Phys.* **66** (1989) 3154.
14. F. YEH and K. W. WHITE, *ibid.* **70** (1991) 4989.
15. L. S. YEOU and K. W. WHITE, *J. Mater. Res.* **7** (1992) 1.
16. B. N. LUCAS, W. C. OLIVER, R. K. WILLIAMS, J. BRYNESTAD and M.E. O'HERN, *ibid.* **6** (1991) 2519.
17. W. H. TUAN, J. M. WU and R. J. BROOK, to be published.
18. J. C. WARST and J. A. NELSON, *J. Amer. Ceram. Soc.* **55** (1972) 109.
19. G. R. ANSTIS, P. CHANTIKUL and B. R. LAWN, *ibid.* **64** (1981) 533.
20. W. WONG-NG, H. F. McMURDIE, B. PARETZKIN, Y. ZHANG, K. K. DAVIS, C. R. HUBBARD, A. L. DRAGOO and J. M. STEWART, *Powder Diff.* **2** (1987) 192.
21. R. W. RICE, "Treatise of Materials Science and Technology", Vol. 11, **11** (Academic Press, New York, 1977) p. 199.
22. W. H. TUAN and R. J. BROOK, *J. Eur. Ceram. Soc.* (1992).
23. R. W. DAVIDGE and T. J. GREEN, *J. Mater. Sci.* **3** (1968) 629.

Received 19 June
and accepted 24 July 1992